Journal for Geometry and Graphics
Volume 7 (2003), No. 1, 89–99.

Manufacturing an Artificial Human Head

Ivana Linkeová

Faculty of Electrical Engineering, Czech Technical University in Prague
Technická 2, 166 27 Prague 6 – Dejvice
email: linkeova@feld.cvut.cz

Abstract. This article focusses on technical applications of mathematical methods from computer graphics — manufacturing free form surfaces on numerically controlled machines by three-axis milling with a spherical-end milling cutter. The procedure of calculating and manufacturing an artificial human head simulator for measurements in physiological acoustics is described in the paper.

Key words: surface fitting, interpolation

MSC 2000: 65U05, 65D17

1. Introduction

The technology of numerically controlled three-axis milling with a spherical-end milling cutter has been used to manufacture the artificial human head simulator. The theoretical pre-production stage of this technology includes a wide range of problems related to the calculation of data (tool path) for numerically controlled machines. The tool path consists of coordinates of endpoints of linear segments through which the center of the spherical part of the cutter goes. Therefore the main task is to generate an offset surface along which the center of the cutter moves by numerically controlled milling. By suitable digitalization of the offset surface, the preliminary data for controlling the movement of the tool can be obtained. Next, it is necessary to arrange the digitized points on a suitable tool path. Finally, it is imperative to check the tool path so that no undercutting of the machining surface will occur.

The following sections demonstrate how in this practical example the problems concerned with the pre-production stage of three-axes milling by a spherical-end milling cutter are solved. The procedure of calculating and manufacturing an artificial human head simulator for measurements in physiological acoustics is explained. The final set consists of the head, of ears and of measuring microphones and it serves for solving pedagogic and research projects at the Faculty of Electrical Engineering, Czech Technical University in Prague.

ISSN 1433-8157/$ 2.50

2. Purpose and use of the artificial human head

The quality of an electroacoustic transducer or of complete electroacoustic systems can be evaluated by classical methods of measuring. By means of the analysis of the input and output signal the transfer function of the measured system is obtained, and thus it is possible to deduce its characteristics. These methods are purely technical, they do not include person's subjective perception of the acoustic signal. Moreover, these methods do not render the influence of a man as an object who is in the acoustic field and whose physical presence affects, through feedback, this field. Because of these reasons and for the purposes of measurements, the models of human heads and torso have been designed and standardized [11].

The set consisting of the model of a human head and torso with electroacoustic apparatus is used for the detection of electroacoustic properties of passive as well as active anti noise buffers, for measuring the transfer functions of stereo headphones. In case the head is completed with an artificial vocal apparatus, it can be used for the optimization and tests of telephone sets. The application of the mentioned models in psychoacoustics when researching binaural perception of the audio signal and its recording is of great importance; then it is used for measuring transfer functions of hearing aids designed for people with impaired hearing, for measuring, recording and analysis of the noise level in the working environment and in automobiles, etc.

Commercially available artificial heads do not solve the problem of modelling the outer auditory canal very extensively. In many cases their measuring microphones are located at the place where the ear canal should start. Therefore the artificial head with an acoustical system that simulates more accurately the external auditory canal has been developed and manufactured.

3. Theoretical part

This section deals with the construction of a mathematical model of the head, with the calculation of an offset surface and the investigation, whether an undercutting of the machining surface occurs.

3.1. Mathematical model of the head

The piecewise interpolation method of patching by Ferguson's 12 vector patches based on mathematical theories of surfaces of computer graphics has been used to construct the mathematical model of the surface of a human head. Input data for this method are the Cartesian coordinates of points which define the free form surface and a pair of tangent vectors at every *definition point* of the surface. The resulting surface passes through all its definition points and consists of smoothly connected parts *(patches)*. The smooth connection of the neighboring patches is ensured by the coincidence of tangent vectors of the corresponding patches at each contact vertex.

3.2. Input data

As a basis for the shape of the head, the definition stated in IEC 959 standard [11] has been used. In this standard the shape of the head is defined by a system of drawn *horizontal section curves*.

For a construction of the mathematical model according to FERGUSON's patching, it was necessary to obtain a spatial network of definition points. The curves were thus taken using a digitization equipment at points determined as the intersection of each section curve with the rays of an auxiliary polar network angularly spaced by 3°. An example for digitizing the section curves is shown in Fig. 1a . All the definition section curves of head and torso obtained by digitalization from the IEC 959 standard are shown in Fig. 1b . The Cartesian coordinates of the obtained points of all the section curves of the head made up the required spatial net of definition points (Fig. 2).

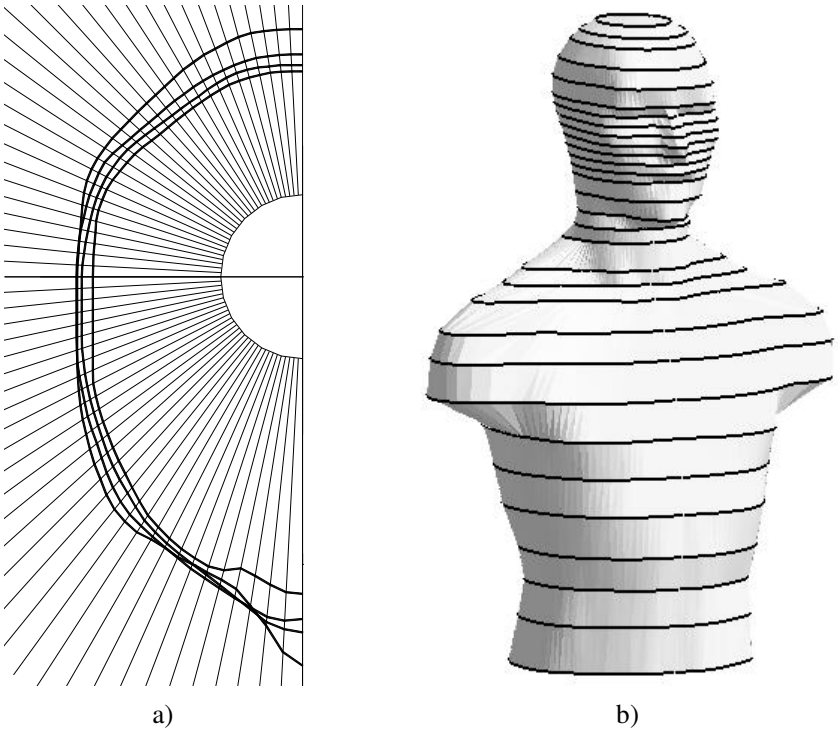

Figure 1: Definition curves of the standardized head and torso
a) digitization of curves, b) all definition curves

3.3. Determination of tangent vectors at definition points

The length and direction of tangent vectors crucially affects the shape of FERGUSON's patch. The determination of the tangent vectors must be carried out before the interpolation surface is calculated, which can pose quite a problem in practice. In this study the tangent vectors have been determined by a method developed for the calculation of pairs of tangent vectors at each definition point so that the shape of the resulting patch optimally reflects the configuration of these points. This method is described in detail in [7] and [5]. In the following paragraph only a brief review is given.

Suppose that in the plane xy the control points are given with position vectors $\mathbf{P}_0$, $\mathbf{P}_1$, $\ldots$, $\mathbf{P}_n$. These control points will be interpolated by a piecewise cubic curve. The segment

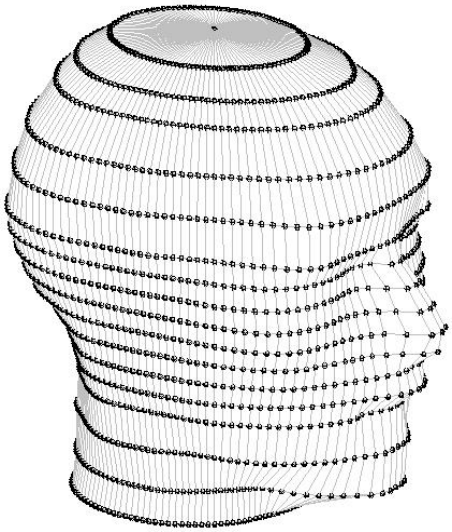

Figure 2: Net of definition points of the head

$\mathbf{P}_i(t)$ of Ferguson's cubic curve is defined as follows:

$$\mathbf{P}_i(t) = \mathbf{T} \cdot \mathbf{F} \cdot \mathbf{M}_i = \begin{bmatrix} t^3 & t^2 & t & 1 \end{bmatrix} \cdot \begin{bmatrix} 2 & -2 & 1 & 1 \\ -3 & 3 & -2 & -1 \\ 0 & 0 & 1 & 0 \\ 1 & 0 & 0 & 0 \end{bmatrix} \cdot \begin{bmatrix} \mathbf{P}_i \\ \mathbf{P}_{i+1} \\ \mathbf{P'}_i \\ \mathbf{P'}_{i+1} \end{bmatrix} \tag{1}$$

where $\mathbf{P}_i(t)$ is the position vector of any point of the curve, $\mathbf{T}$ depends on the parameter t, $\mathbf{F}$ is the matrix of coefficients of Ferguson's *blending functions* and $\mathbf{M}_i$ is a vector of geometric coefficients. The unknown tangent vectors required to calculate eq. (1) are determined as follows:

$$\begin{aligned} \mathbf{P'}_0 &= -\tfrac{3}{2}\mathbf{P}_0 + 2\mathbf{P}_1 - \tfrac{1}{2}\mathbf{P}_2 \\ \mathbf{P'}_i &= d_i \cdot \tfrac{1}{2}(\mathbf{P}_{i+1} - \mathbf{P}_{i-1}) \\ \mathbf{P'}_n &= \tfrac{1}{2}\mathbf{P}_{n-2} - 2\mathbf{P}_{n-1} + \tfrac{3}{2}\mathbf{P}_n \end{aligned} \tag{2}$$

The coefficient d_i represents the *correction coefficient* of the length of calculated tangent vectors. It is a linear function of the angle $\gamma_i = \angle\mathbf{P}_{i-1}\mathbf{P}_i\mathbf{P}_{i+1}$ between two following chords (Fig. 3a):

$$d_i = d_{\min} + \frac{d_{\max} - d_{\min}}{180} \cdot (180 - \gamma_i) \tag{3}$$

where the values of $d_{\max}$ and $d_{\min}$ are empirically set to $d_{\max} = 3$, $d_{\min} = 1$. d_i reaches the maximum value 1, which corresponds to the angle $\gamma_i = 180°$, and the minimum value 0.3 for the angle $\gamma_i = 0°$. This method of determining tangent vectors and the adjustment of their length shows minimal undesirable waving among the definition points, overshootings in the vicinity of the definition points are considerably limited, and C^1 continuity is ensured among individual parts of Ferguson's cubic curves, since the tangent vectors at the endpoints are identical (Fig. 3b).

3.4. Construction of a mathematical model for a free form surface

The above mentioned method of determining the tangent vectors at the definition points can be used for the construction of piecewise interpolation surfaces such that a tensor product

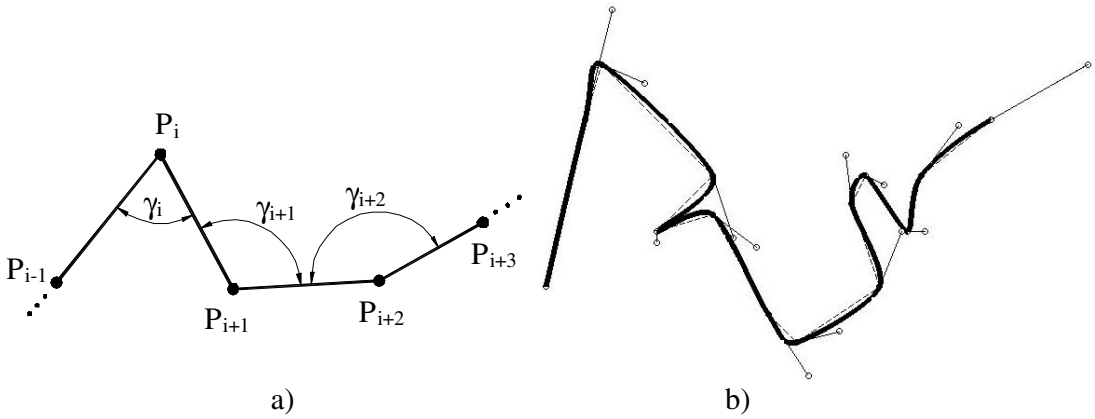

Figure 3: Determination of tangent vectors
a) determination of the angle γ_i, b) interpolation curve and tangent vectors

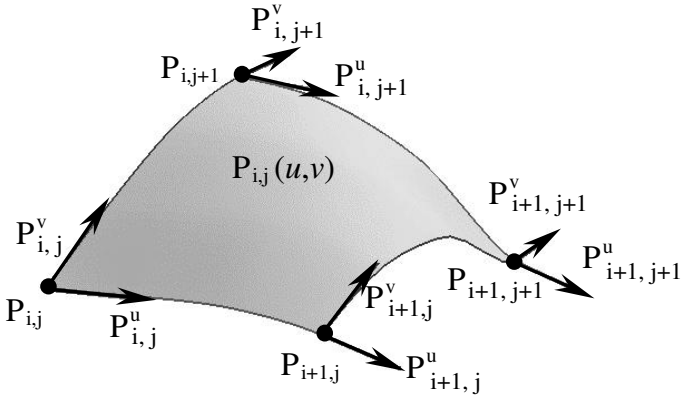

Figure 4: Ferguson's 12 vector patch

approach is possible. A Ferguson's 12 vector patch is given as

$$\mathbf{P}_{i,j}(u,v) = \mathbf{U} \cdot \mathbf{F} \cdot \mathbf{M}_{i,j} \cdot \mathbf{F}^{\mathrm{T}} \cdot \mathbf{V}^{\mathrm{T}} \tag{4}$$

where $\mathbf{P}_{i,j}(u,v)$ is the position vector of a point of the patch, $\mathbf{U} = \left[\begin{array}{cccc} u^3 & u^2 & u & 1 \end{array}\right]$ and $\mathbf{V} = \left[\begin{array}{cccc} v^3 & v^2 & v & 1 \end{array}\right]$ depend on the parameters u and v, and $\mathbf{F}$ is the matrix of coefficients of Ferguson's blending functions (1). The mapping matrix $\mathbf{M}_{i,j}$ of the patch has the form:

$$\mathbf{M}_{i,j} = \left[\begin{array}{cccc} \mathbf{P}_{i,j} & \mathbf{P}_{i,j+1} & \mathbf{P}^v_{i,j} & \mathbf{P}^v_{i,j+1} \\ \mathbf{P}_{i+1,j} & \mathbf{P}_{i+1,j+1} & \mathbf{P}^v_{i+1,j} & \mathbf{P}^v_{i+1,j+1} \\ \mathbf{P}^u_{i,j} & \mathbf{P}^u_{i,j+1} & \mathbf{0} & \mathbf{0} \\ \mathbf{P}^u_{i+1,j} & \mathbf{P}^u_{i+1,j+1} & \mathbf{0} & \mathbf{0} \end{array}\right]$$

where $\mathbf{P}_{i,j}$, $\mathbf{P}_{i+1,j}$, $\mathbf{P}_{i,j+1}$, $\mathbf{P}_{i+1,j+1}$ are position vectors of the patch vertices. The tangent vectors $\mathbf{P}^u_{i,j}$, $\mathbf{P}^u_{i+1,j}$, $\mathbf{P}^u_{i,j+1}$, $\mathbf{P}^u_{i+1,j+1}$ and $\mathbf{P}^v_{i,j}$, $\mathbf{P}^v_{i+1,j}$, $\mathbf{P}^v_{i,j+1}$, $\mathbf{P}^v_{i+1,j+1}$ are the tangent vectors at the vertices in u- and v-direction, respectively (Fig. 4). The zero mixed partial derivatives at the vertices of the Ferguson's 12 vector patch are represented by four zero vectors in the matrix $\mathbf{M}_{i,j}$.

The construction of the whole interpolation surface is shown in Fig. 5, where a detail of the face is depicted. The set of definition points of the free form surface is arranged into

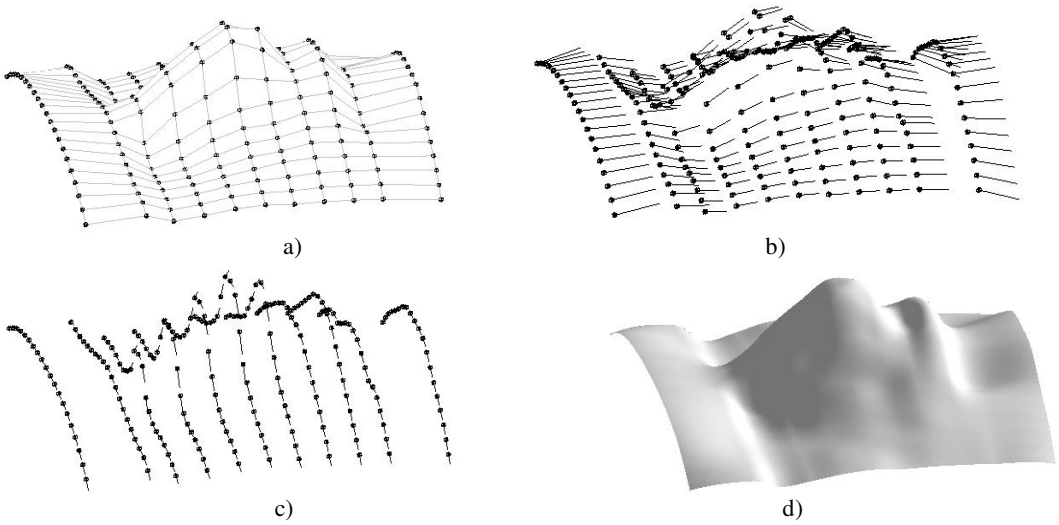

Figure 5: Construction of the interpolation surface
a) net of definition points, b) tangent vectors in u-direction,
c) tangent vectors in v-direction, d) interpolation surface

Figure 6: Mathematical model of a human head

a matrix (Fig. 5a). It can be seen as two families of curves. The tangent vectors at each definition point for both directions calculated according to (2) are shown in Fig. 5b,c . Thus the pair of tangent vectors required for calculating FERGUSON's patch is given. The resulting piecewise interpolation surface is depicted in Fig. 5d . The mathematical model of the human head is shown in Fig. 6.

3.5. Offset surface approximation

The definition of the offset surface $\mathbf{P}^{\mathrm{E}}(u, v)$ corresponding to the surface $\mathbf{P}(u, v)$ is given by

$$\mathbf{P}^{\mathrm{E}}(u, v) = \mathbf{P}(u, v) + \alpha \cdot \mathbf{n}(u, v). \tag{5}$$

The offset surface $\mathbf{P}^{\mathrm{E}}(u, v)$ is constructed in such a way that at every point of the surface $\mathbf{P}(u, v)$ the constant distance α is put on the oriented normal $\mathbf{n}(u, v)$. The end points of the

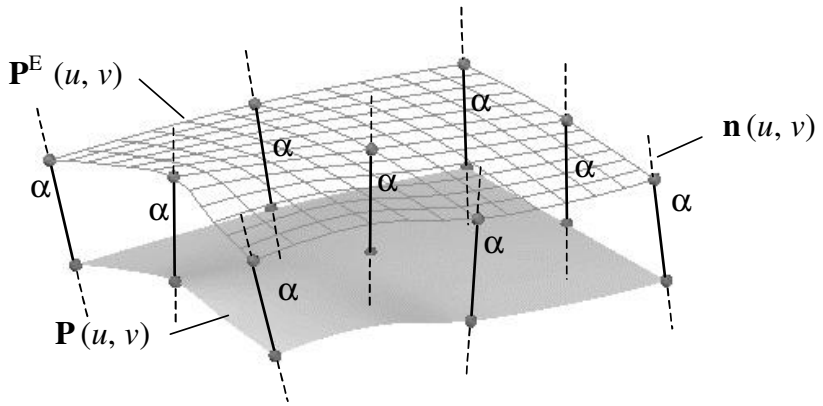

Figure 7: Definition of the offset surface

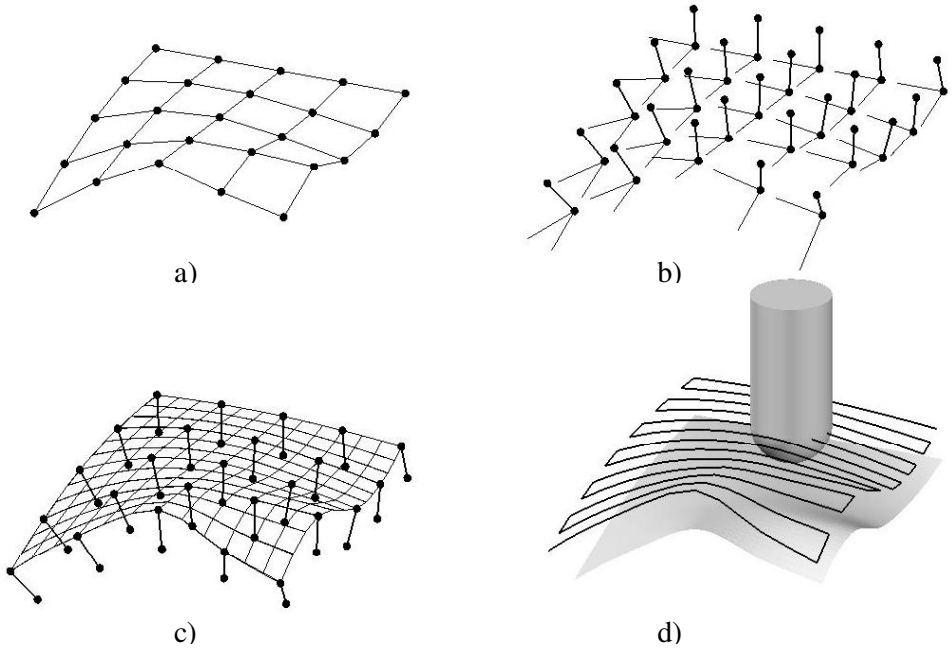

Figure 8: Construction of the offset surface
a) net of definition points, b) tangent and normal vectors at definition points,
c) digitization of the offset surface, d) tool path

normals define the offset surface $\mathbf{P}^{\mathrm{E}}(u, v)$ (Fig. 7). Offset surfaces have common normals and parallel tangent planes at corresponding points.

Provided that the pair of tangent vectors has been calculated, the construction of the offset surface can be simplified. If we carry out the vector product of the pair of calculated tangent vectors at each point, we get a vector perpendicular to them (Fig. 8b). In the distance equal to the radius of the cutting tool, there is a point which can be interpreted as the new definition point. This point now defines the offset surface. We shall use the same algorithms and calculate the offset surface as the interpolation surface, which goes through the new definition points (Fig. 8c). This new interpolation surface represents a mathematical model of the offset surface along which the center of the cutter moves by numerically controlled milling. Next, the digitization of the constructed offset surface follows. The digitized points are arranged in a suitable way and the tool path is created (Fig. 8d).

The accuracy of the offset surface significantly influences the final accuracy of the machined surface, but it is limited by the technological accuracy. In order to evaluate the accuracy and reliability of this offset surface approximation, the points lying on the analytic surfaces (sphere [6] and torus [5]) were tested. The accuracy of the mathematical model is significantly affected by the number of input points and by the distances between neighbouring input points. Therefore, several nets of input data differing in the number and distribution of points were calculated. In [6] and [5], the following results were obtained: if the relative distance between two neighbouring input points is smaller than 0.05 the relative approximation error is approximately 10^{-6} for the sphere (of radius 1) and 10^{-5} for the torus (circle of radius 0.5 revolves about the axis at the distance of 1). The above-mentioned method can be considered to be sufficiently precise with respect to the technological accuracy (the producer specifies the least programmable step of about 0.001 mm and the least repeated accuracy of positioning of about 0.005 mm for dimensions given by the size of the NC milling machines working space of about 1000 mm).

3.6. Undercuttings at the machining surface

One part of determining the offset surface is also to check possible undercuttings caused by the dimensions and the geometry of the cutting tool, in case of milling the internal edges and corners. The undercutting occurs during milling when the radius of the cutting tool is larger than the minimal normal curvature of the objective surface.

The tool path finally represents a spatial polygonal line which consists of elementary linear segments. The planar situation is depicted in Fig. 9. The endpoints of the polygonal line approximating the offset curve are denoted by $\mathbf{R}_i$, $i = 1, \ldots, 8$; the endpoints of the polygonal line interpolating the machining surface are denoted by $\mathbf{S}_i$. If the tool runs through all the points $\mathbf{R}_i$, $i = 1, \ldots, 8$, an undercutting occurs. The shape of the machining surface is deformed. If the tool leaves out the dashed part of the path, then undercutting does not occur. It is necessary to use the tool with a sufficiently small radius to machine the surface in the ignored area.

A simple approach for eliminating undercuttings has been chosen. The algorithm consists of the following steps (see Fig. 9):

1. Find the points $\mathbf{R}_i$ whose z-coordinates reach a (local) minimum.
2. Place the tool centre $\mathbf{C}_1$ at all points determined in step 1 (e.g., $\mathbf{R}_5$ in Fig. 9).
3. If there are some points $\mathbf{S}_i$ in the tool space $\mathbf{T}_1$ (including the tool boundary), then undercutting occurs (this happens for the points $\mathbf{S}_3, \ldots, \mathbf{S}_6$ in Fig. 9) and the algorithm continues from step 5.
4. If there are points $\mathbf{S}_i$ on the tool boundary only, but not in the tool space, undercutting does not occur. The algorithm ends.
5. Among the points found in step 3, select the point which satisfies the following two conditions:
   (a) The distance between the point and the tool centre $\mathbf{C}_1$ is minimal.
   (b) The z-coordinate of the point is smaller than the z-coordinate of the tool centre $\mathbf{C}_1$. (In Fig. 9 $\mathbf{S}_4$ satisfies both condition a and b).

   Once such a point is found, the current position of the tool centre $\mathbf{C}_1 = \mathbf{R}_5$ is removed from the tool path.

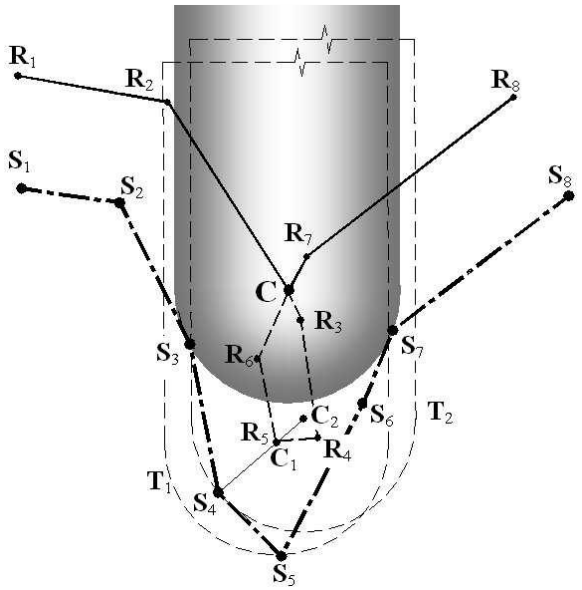

Figure 9: Elimination of undercutting

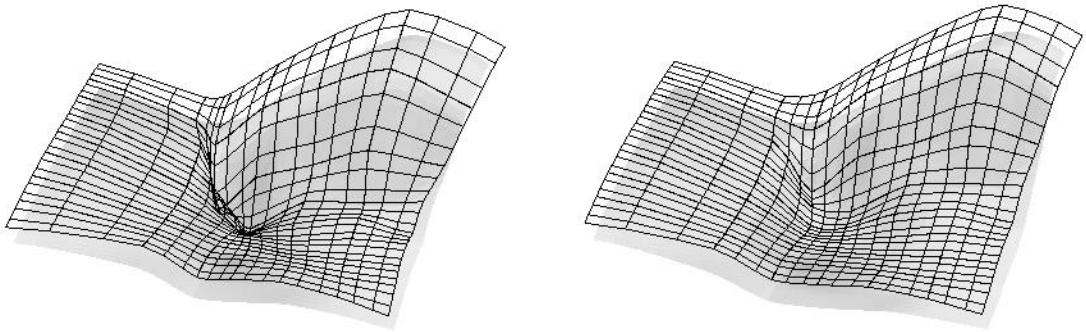

Figure 10: Recalculation of the offset surface to eliminate undercuttings
a) original offset surface, b) recalculated offset surface

6. The point removed in 5b is replaced by a new point $\mathbf{C}_2$, which lies on the connecting line $\mathbf{S}_4\mathbf{R}_5$ (of the point found in step 5 and of the removed point) at the distance equal to the radius of the tool from $\mathbf{S}_4$. The tool centre is placed into the new point.

7. Now, the previous steps 3 to 6 are repeated, new possible positions of the tool centre are found, new corresponding tool spaces are investigated until condition 4 is achieved. The final position of the tool centre $\mathbf{C}$ is found, the undercutting caused by $\mathbf{R}_5$ is eliminated.

8. The algorithm starts again from step 1, the next points $\mathbf{R}_i$ whose z-coordinates reach the (local) minimum are found ($\mathbf{R}_4$ in Fig. 9).

9. The algorithm ends when all points $\mathbf{R}_i$ have fulfilled condition 4.

This algorithm was applied to generate the tool path for manufacturing an artificial human head [8]. Fig. 10 shows two details of the region around the eyes. The form of the calculated offset surface is depicted in Fig. 10a, and the recalculated variant of this surface with removed undercutting is shown in Fig. 10b.

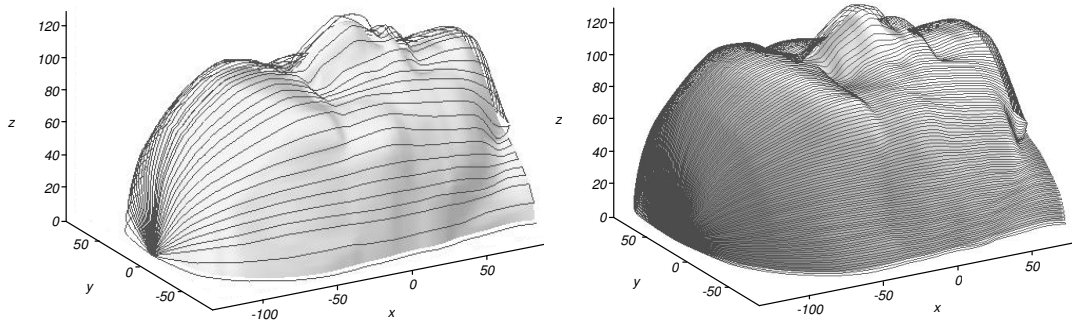

Figure 11: Manufacturing the front part of the head

4. Manufacturing the artificial head

The final model of the head was produced as a hollow casting from plaster of paris. The mould was manufactured according to the milled model from polystyrene foam.

The milled model of the head consists of front and back parts. Both parts of the head were milled from the blocks of the material glued on a wooden support plate, which could be clamped to the work bench of the milling machine. Fig. 11 shows the manufacturing procedure for the front part of the head. For removing the excessive material, several roughing programmes have been generated. The material allowance of approx. 1 mm measured on the normal to the surface, remained on the whole surface after the last roughing cycle (Fig. 11a). The final tool path is depicted in the Fig. 11b). The distance of the individual paths was chosen to guarantee a manufacturing tolerance. In the final phase of the calculation, the analysis of the tool path was performed and the patches of the area where undercuttings can occur (parts of the eyes, nose and mouth) were recalculated.

4.1. Final set

The final set consists of the head, of ears and of measuring microphones (Fig. 12). The pinnae are made of resin and it is glued to the mass of the head with silicon glue. The modules carrying the microphones are inserted into openings in the structure of the head in a position which ensures an appropriate function of model. The output signal is led by a cable, which goes through axes of the head and torso. The resulting behaviour of this set is close to that of the human body. The set is used in an anechoic chamber located in the Acoustic Laboratory of the Department of Physics.

5. Conclusion

The model of the artificial head was made according to international standards and their industrial embodiments. The technology of three-axis milling by a numerically controlled milling cutter has been used to manufacture the initial model of the head. The problems concerned with the theoretical pre-production stage of this technology was described in the paper.

The algorithms for calculating the mathematical model of the manufactured surface and the offset surface, the generation of the tool path and removing undercuttings were programmed in Visual Basic for applications in Microsoft Excel software. The majority of figures

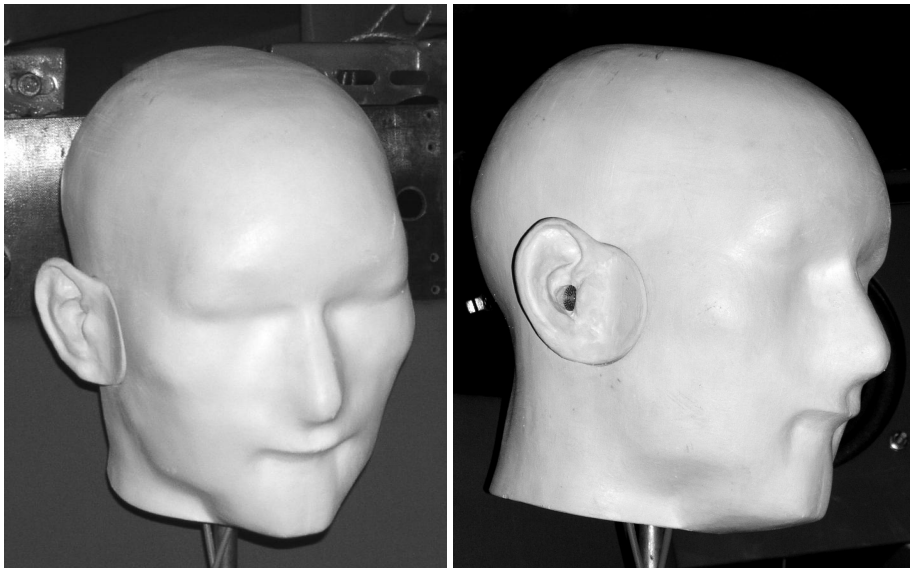

Figure 12: Final set

was obtained by means of MAPLE software.

References

[1] M. Brothánek, O. Jiříček: *Formating of Zones of Quiet around a Head Simulator*. Active 2002, University of Southampton, 117–121 (2002).

[2] J.D. Foley, A. Van Dam, S.K. Feiner, J.F. Hughes: *Computer Graphics: Principles and Practice*. Addison-Wesley Publ. Company, 1993.

[3] G. Glaeser, J. Wallner, H. Pottmann: *Collision-free 3-Axis Milling and Selection of Cutting Tools*. Computer-Aided Design **31**, 225–232 (1999).

[4] L. Husník: *Artificial Head for Measurements in Physiological Acoustics*. Workshop 2001, CTU Prague, 374–375 (2001).

[5] I. Linkeová: *Offset Surfaces Construction*. FAIM 2002, Oldenbourg Wissenschaftsverlag, 1063–1072 (2002).

[6] I. Linkeová: *Mathematical Model of Offset Surfaces*. Scientific Bulletin of the Technical University of Lodz, 2001, TU v Lodzi, 211–216 (2001).

[7] I. Linkeová: *Determination of Tangent Vectors in Construction of Ferguson Interpolation Curves and Surfaces*. Acta Polytechnica **40**, no. 5-6/2000, 27–32 (2001).

[8] I. Linkeová: *Construction, Manufacturing and Measuring of Free Form Surfaces*. Thesis, CTU Prague 1999.

[9] T. Maekawa: *An Overview of Offset Curves and Surfaces*. Computer-Aided Design **31**, 165–173 (1999).

[10] L. Piegl, W. Tiller: *The NURBS Book*. Springer-Verlag 1997.

[11] IEC 959: *Provisional Head and Torso Simulator for Acoustic Measurements on Air Conduction Hearing Aids*. 1990.

Received March 1, 2003; final form July 17, 2003